Absence of IFN-γ accelerates thrombus resolution through enhanced MMP-9 and VEGF expression in mice

Mizuho Nosaka,[1] Yuko Ishida,[1] Akihiko Kimura,[1] Yumi Kuninaka,[1] Masanori Inui,[2] Naofumi Mukaida,[3] and Toshikazu Kondo[1]

[1]Department of Forensic Medicine, and [2]Department of Immunology, Institute of Advanced Medicine, Wakayama Medical University, Wakayama, Japan. [3]Division of Molecular Bioregulation, Cancer Research Institute, Kanazawa University, Kanazawa, Japan.

Deep vein thrombosis (DVT) is a major cause of pulmonary thromboembolism, a leading cause of death in individuals with DVT. Several lines of evidence indicate proinflammatory cytokines such as TNF-α are involved in thrombus formation and resolution, but the roles of IFN-γ remain unclear. To address this issue, we performed ligation of the inferior vena cava to induce DVT in WT and IFN-γ–deficient (*Ifng*$^{-/-}$) mice. In WT mice, intrathrombotic IFN-γ levels were elevated progressively as the postligation interval was extended. Thrombus size was substantially smaller at 10 and 14 days in *Ifng*$^{-/-}$ mice than in WT mice. Intrathrombotic collagen content was remarkably reduced at more than 10 days after the ligation in *Ifng*$^{-/-}$ mice compared with WT mice. The expression and activity of MMP-9, but not MMP-2, was higher at the late phase in *Ifng*$^{-/-}$ mice than in WT mice. Moreover, intrathrombotic recanalization was increased in *Ifng*$^{-/-}$ mice, with enhanced *Vegf* gene expression, compared with that in WT mice. Activation of the IFN-γ/Stat1 signal pathway suppressed PMA-induced *Mmp9* and *Vegf* gene expression in peritoneal macrophages. Furthermore, administration of anti–IFN-γ mAbs accelerated thrombus resolution in WT mice. Collectively, these findings indicate that IFN-γ can have detrimental roles in thrombus resolution and may be a good molecular target for the acceleration of thrombus resolution in individuals with DVT.

Introduction

Deep vein thrombosis (DVT) is multifactorial and often results from a combination of risk factors such as genetic conditions, obesity, drugs, pregnancy, aging, trauma, and malignancy (1–3). DVT is frequently complicated with severe morbidity, leading sometimes to mortality (4–6). Indeed, the American Heart Association reported that approximately 2,000,000 people annually suffered from DVT and that 200,000 of these died from pulmonary thromboembolism, one of the severe complications arising from DVT, in the United States alone. Thus, in order to minimize the mortality of DVT-related pulmonary thromboembolism, accurate diagnosis and prompt therapy for DVT are necessary (5). Standard treatments for DVT aim to prevent death from pulmonary embolism, propagation of the thrombus, and recurrence of venous thromboembolism. At present, anticoagulation with either unfractionated or low–molecular weight heparin, or warfarin is used to inhibit thrombus extension, to allow natural resolution, and to slowly reduce and organize the existing thrombus (4). However, anticoagulation cannot accelerate natural thrombus resolution and reciprocally increases the risk of bleeding. Moreover, any treatment modalities have not been developed to directly lyse thrombus until the present.

The pathogenesis of venous thrombosis involves 3 factors, referred to as Virchow's triad; endothelial damages, stasis or turbulence of blood flow, and blood hypercoagulability. Damage to the vessel wall prevents the endothelium from inhibiting coagulation and initiating local fibrinolysis. Venous stasis inhibits the clearance and dilution of activated coagulation factors. Finally, congenital or acquired thrombophilia promotes coagulation. Several lines of evidence indicate the involvement of proinflammatory cytokines and chemokines in the thrombus formation and resolution (7–10). Indeed, TNF-α and IL-1β can potently activate endothelial cells, increase the expression of adhesion molecules by endothelial cells, and promote thrombosis (11–15). Moreover, TNF-α and IL-1β can induce the expression of chemokines, which can activate leukocytes to accelerate thrombus resolution and intrathrombotic neovascularization (16–18).

IFN-γ exerts pleiotropic effects on NK cells and macrophages, including enhancement of their antiviral and bactericidal activities and upregulation of MHC class II expression on macrophages (19). Moreover, accumulating evidence implicates IFN-γ as a major mediator in various types of disease models (20–25). Furthermore, we previously determined that the IFN-γ/Stat1 signal pathway played an important role in skin wound healing by regulating VEGF expression and the TGF-β signaling pathway (23). The thrombus resolution process resembles wound healing, with the injury nidus being the clot, followed by leukocyte recruitment and eventually matrix accumulation. Indeed, we immunohistochemically detected IFN-γ protein in deep vein thrombi taken from autopsy cases (Supplemental Figure 1; supplemental material available online with this article; doi:10.1172/JCI40782DS1). These observations prompted us to explore the pathophysiological roles of IFN-γ in the process of thrombus formation and resolution in a stasis-induced thrombosis model by the use of IFN-γ–deficient (*Ifng*$^{-/-}$) mice.

We demonstrated that thrombus resolution was accelerated in *Ifng*$^{-/-}$ mice compared with WT mice without any differences in thrombosis formation. Moreover, the expression of an enzyme with collagenolytic activity, MMP-9, was enhanced at mRNA and enzymatic activity

Authorship note: Mizuho Nosaka and Yuko Ishida contributed equally to this work.
Conflict of interest: The authors have declared that no conflict of interest exists.
Citation for this article: *J Clin Invest.* 2011;121(7):2911–2920. doi:10.1172/JCI40782.

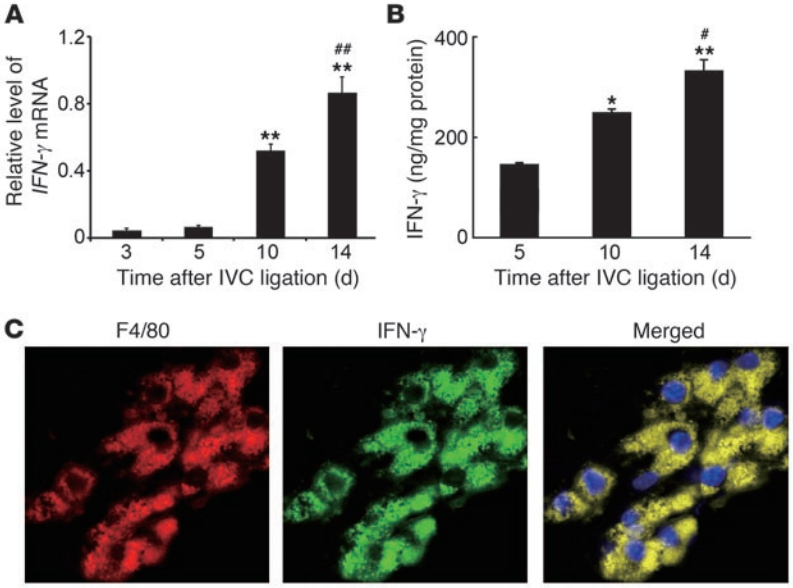

Figure 1
Intrathrombotic IFN-γ expression in WT mice after IVC ligation. (**A**) *Ifn*γ gene expression was examined by real-time RT-PCR as described in Methods. All values represent mean ± SEM (n = 6). $^{**}P < 0.01$, versus day 3; $^{\#\#}P < 0.01$, versus day 10. (**B**) Intrathrombotic IFN-γ protein contents were determined at the indicated time intervals after IVC ligation as described in Methods. All values represent mean ± SEM (n = 6). $^{**}P < 0.01$, versus day 5; $^{*}P < 0.05$, versus day 5; $^{\#}P < 0.05$, versus day 10. (**C**) A double-color immunofluorescence analysis of IFN-γ–expressing cells in the thrombus. The samples were immunostained with the combination of anti-F4/80 mAbs and anti–IFN-γ pAbs as described in Methods. The fluorescent images were digitally merged in the right panel. Representative results from 6 independent experiments are shown here. Original magnification, ×400. Blue, nuclear staining by DAPI.

levels in *Ifng*$^{-/-}$ mice compared with WT mice. Furthermore, intrathrombotic vascular channels were increased with enhanced VEGF expression in *Ifng*$^{-/-}$ mice, compared with WT mice. These observations imply that IFN-γ plays a detrimental role in thrombus resolution by suppressing MMP-9 and VEGF expression.

Results

Intrathrombotic IFN-γ expression after the inferior vena cava ligation (IVC). We examined intrathrombotic *Ifng* gene expression in WT mice at 3, 5, 10, and 14 days after the IVC ligation. *IFN-γ* mRNA was consistently detected in thrombi and its expression was elevated progressively as thrombi aged (Figure 1A). Likewise, IFN-γ proteins were detected in thrombi and increased progressively after the IVC ligation (Figure 1B). Moreover, double-color immunofluorescence analyses detected IFN-γ mainly in F4/80-positive macrophages (Figure 1C). These observations implied that IFN-γ was produced in thrombi mainly by infiltrating macrophages.

Enhanced thrombus resolution in the absence of IFN-γ. In order to explore the pathophysiological roles of IFN-γ in the development of stasis-induced venous thrombus, we compared thrombus formation between WT and *Ifng*$^{-/-}$ mice. In WT mice, venous thrombi developed progressively until 5 days but remained similar in size until 10 days after the IVC ligation, decreasing thereafter (Figure 2A). In *Ifng*$^{-/-}$ mice, thrombi started to reduce in size 10 days after the IVC ligation (Figure 2, A and B) and were smaller than those in WT mice 14 days after the IVC ligation. Because intrathrombotic collagen contents can reflect thrombus mass (18), we determined intrathrombotic collagen contents by the use of histopathological and biochemical methods. In *Ifng*$^{-/-}$ mice, intrathrombotic collagen area was remarkably reduced compared with that in WT mice (Figure 2, C and D, and Supplemental Figure 2). Similarly, intrathrombotic contents of both collagen and hydroxyproline, a major component of collagen, were significantly diminished in *Ifng*$^{-/-}$ mice later than 10 days after the IVC ligation, compared with WT mice (Figure 2, E and F). These observations implied that the absence of IFN-γ could accelerate the resolution of stasis-induced venous thrombi.

The absence of IFN-γ had no effects on intrathrombotic leukocyte recruitment and the expression of chemokines, tPA, uPA, and PAI. The potential contribution of intrathrombotic leukocytes to the resolution of venous thrombi (12–18) prompted us to investigate the effects of IFN-γ deficiency on intrathrombotic leukocyte recruitment. Myeloperoxidase (MPO)-positive neutrophils infiltrated thrombi in WT and *Ifng*$^{-/-}$ mice to similar extents, reaching a maximal level at 1 day after the IVC ligation and decreasing gradually thereafter (Figure 3, A and C). Likewise, F4/80-positive macrophages infiltrated thrombi in WT and *Ifng*$^{-/-}$ mice to similar extents, reaching a maximal level at 5 days after the IVC ligation and decreasing gradually thereafter (Figure 3, B and D). Similar tendencies were also observed on the infiltration of CD11b-positive cells (data not shown). In line with this, we further detected the gene expression of several chemokines including *CXCL1/KC*, *CXCL2/MIP-2*, *CCL2/MCP-1*, and *CCL3/MIP-1*α to similar extents in WT and *Ifng*$^{-/-}$ mice (Supplemental Figure 3). Because the plasmin system is also essential for cell migration and subsequent thrombus resolution (26–28), we examined the intrathrombotic gene expression of tissue-type plasminogen activator (*tPA*), urokinase-type plasminogen activator (*uPA*), and plasminogen activator inhibitor-1 (*PAI-1*). We failed to detect any significant differences in the expression of these genes between WT and *Ifng*$^{-/-}$ mice at any time point after IVC ligation (Figure 4). Collectively, the absence of IFN-γ had little, if any, effects on intrathrombotic expression of chemokines, *tPA*, *uPA*, and *PAI-1*, and subsequent leukocyte recruitment.

Enhanced enzymatic activity of MMP-9 but not MMP-2 in Ifng$^{-/-}$ *mice.* MMP-2 and MMP-9 have crucial roles in collagenolysis during thrombus resolution (18). Thus, we examined the intrathrombotic gene expression and the enzymatic activity of MMP-2 and MMP-9. *MMP-2* mRNA and enzymatic activities were detected consistently in thrombi at similar levels in WT and *Ifng*$^{-/-}$ mice (Figure 5, A, C, and D). *Mmp9* gene expression was detected in thrombi of WT mice, reaching the maximal level at 5 days after the IVC ligation and declining thereafter (Figure 5B). In *Ifng*$^{-/-}$ mice, *MMP-9* mRNA was detected, to a similar extent, at 5 days, but its levels remained similar until 14 days after the IVC ligation (Figure 5B). Likewise, the enzymatic activities of MMP-9 remained at similar levels in *Ifng*$^{-/-}$ mice until 14 days after the IVC ligation, whereas its activities decreased in WT mice at 10 days after the ligation

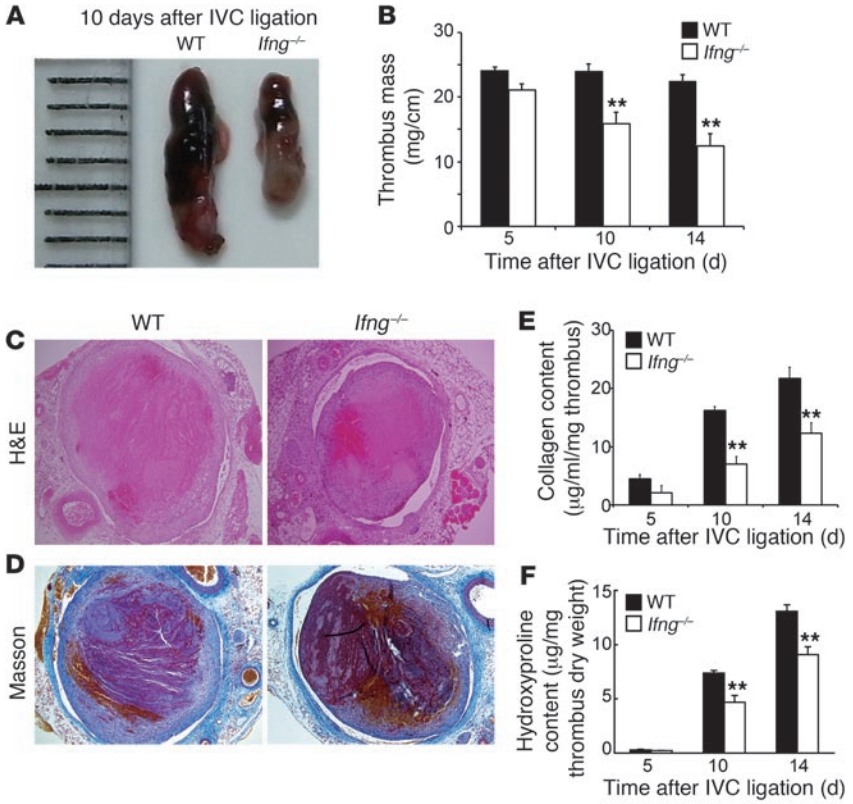

Figure 2
Stasis-induced deep vein thrombus in WT and *Ifng*$^{-/-}$ mice. (**A**) Macroscopic appearance of intravenous thrombi in WT and *Ifng*$^{-/-}$ mice 10 days after the IVC ligation. Representative results from 6 independent animals are shown here. (**B**) Thrombus weights of WT and *Ifng*$^{-/-}$ mice at the indicated time intervals after IVC ligation. All values represent the mean ± SEM (n = 6). $^{**}P < 0.01$, *Ifng*$^{-/-}$ versus WT. (**C** and **D**) Histopathological analyses of venous thrombi obtained from WT and *Ifng*$^{-/-}$ mice 10 days after IVC ligation. Thrombus samples were stained with H&E (**C**) or Masson trichrome solution (**D**). Representative results from 6 independent experiments are shown here. Original magnification, ×100. (**E** and **F**) Intrathrombotic contents of collagen and HP, a major component of collagen, of WT and *Ifng*$^{-/-}$ mice at the indicated time intervals after IVC ligation. All values represent the mean ± SEM (n = 6). $^{**}P < 0.01$, *Ifng*$^{-/-}$ versus WT.

(Figure 5, C and E). Consistently, later than 10 days after the IVC ligation, intrathrombotic MMP-9–positive cell numbers were higher in *Ifng*$^{-/-}$ mice than in WT mice (Figure 6, A and B). Moreover, a double-color immunofluorescence analysis demonstrated that F4/80-positive macrophages were a main cellular source of MMP-9 (Figure 6C). Collectively, these observations would imply that IFN-γ might play a detrimental role in thrombus resolution by suppressing the expression of MMP-9 but not MMP-2 in macrophages present in the thrombus.

Enhanced intrathrombotic recanalization in Ifng$^{-/-}$ *mice.* Intrathrombotic recanalization was presumed to be essential for thrombus resolution (29–31). The number of intrathrombotic vWF-positive channels was significantly increased at 10 and 14 days in *Ifng*$^{-/-}$ mice compared with WT mice (Figure 7, A and B). Moreover, we examined blood flow within and around the thrombosed IVC by the use of laser Doppler imaging (18). At 5 days after IVC ligation, there were no significant differences in the blood flow of thrombosed IVC between WT and *Ifng*$^{-/-}$ mice. However, at 10 and 14 days after IVC ligation, the blood flow was recovered in *Ifng*$^{-/-}$ to larger extents than in WT mice (Figure 7C). Furthermore, intrathrombotic gene expression of *VEGF*, a potent angiogenic factor, was significantly enhanced in *Ifng*$^{-/-}$ mice compared with WT mice (Figure

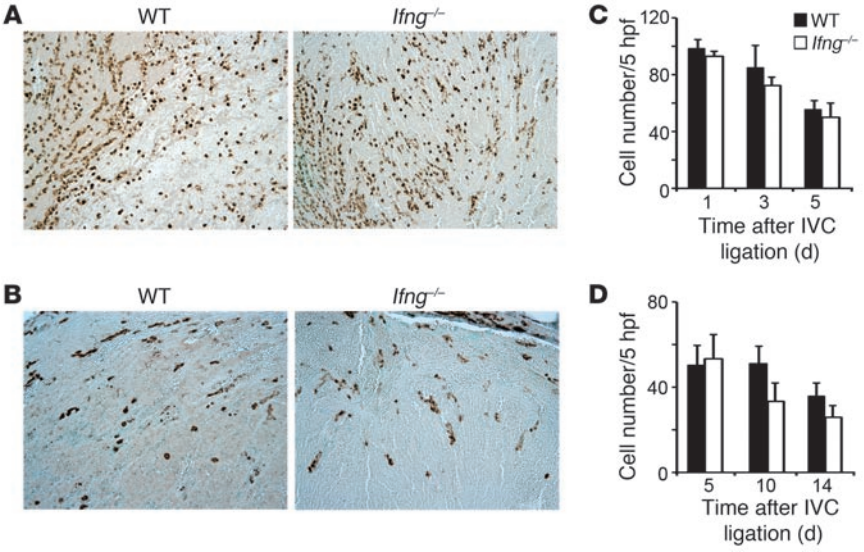

Figure 3
Enumeration of intrathrombotic leukocytes in WT and *Ifng*$^{-/-}$ mice. (**A** and **B**) Immunohistochemical analysis was performed using anti-MPO pAbs at day 1 (**A**) or anti-F4/80 mAbs at day 5 (**B**) in venous thrombus samples from WT and *Ifng*$^{-/-}$ mice. Original magnification, ×400. Representative results from 6 independent experiments are shown here. The numbers of neutrophils (**C**) and macrophages (**D**) were determined as described in Methods. All values represent the mean ± SEM (n = 6 animals).

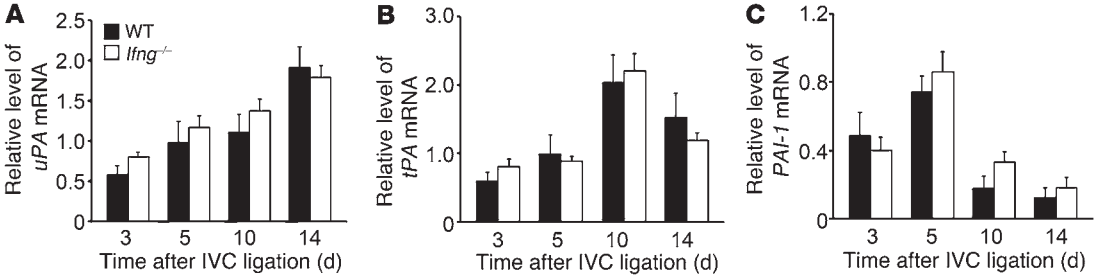

Figure 4
Intrathrombotic gene expression of *tPA*, *uPA*, and *PAI-1* determined by real-time RT-PCR. All values represent the mean ± SEM (n = 6 animals).

7D). A double-color immunofluorescence analysis demonstrated that F4/80-positive macrophages were a main cellular source of VEGF (Figure 7E). These observations implied that the lack of IFN-γ might increase intrathrombotic recanalization at least partly through enhanced *Vegf* gene expression in macrophages.

Effects of an MMP inhibitor on thrombus resolution. There are controversies on the roles of MMP-9 in thrombus formation and resolution (18, 32). Hence, in order to define precisely the roles of enhanced MMP expression in this process, we examined the effects of an MMP inhibitor on thrombus resolution. The administration of an MMP-2/9 inhibitor impaired thrombus resolution, as evidenced by thrombus mass and intrathrombotic collagen contents, and thrombosed blood flow (Figure 8, A to C), whereas it had no effects on intrathrombotic *Vegf* gene expression (Figure 8D). These observations implied that MMPs have important roles in collagenolysis and angiogenesis during thrombus resolution, with few effects on VEGF expression.

IFN-γ/Stat1 signal pathway negatively regulated the gene expression of MMP-9 and VEGF in macrophages. Our in vivo observations suggest that IFN-γ could suppress the gene expression of MMP-9 and VEGF in intrathrombotic macrophages. To validate this hypothesis, we examined the effects of IFN-γ on the gene expression of *MMP-9* and *VEGF* in WT mouse–derived peritoneal macrophages. PMA significantly enhanced *Mmp9* and *Vegf* gene expression in macrophages (Figure 9, A and B). IFN-γ significantly suppressed PMA-induced gene expression of *MMP-9* and *VEGF* and increase in Stat1 phosphorylation (Figure 9, A–D). Reciprocally, these IFN-γ effects were abrogated by AG490, a JAK2 inhibitor (Figure 9, A to D). These observations strongly implied that the IFN-γ/Stat1 signal pathway negatively regulated *Mmp9* and *Vegf* gene expression in macrophages.

Effects of anti–IFN-γ mAbs on thrombus resolution. We finally examined the therapeutic effects of anti–IFN-γ mAbs on the resolution of stasis-induced venous thrombi. When WT mice received anti–IFN-γ mAbs or control IgG at 4, 8, and 12 days after the IVC ligation, thrombus mass and intrathrombotic collagen contents were smaller in anti–IFN-γ mAb–treated WT mice than control IgG-treated WT ones (Figure 10, A and B). Consistently, blood flow was larger in anti–IFN-γ mAb–treated WT mice than in control IgG-treated WT ones (Figure 10C). Concomitantly, the intrathrombotic gene expression of *MMP-9* and *VEGF* was significantly higher in the anti–IFN-γ mAb–treated group than in the control IgG-treated group (Figure 10, D and E). Moreover, the administration of anti–IFN-γ mAbs did not cause any abnormalities in coagulation func-

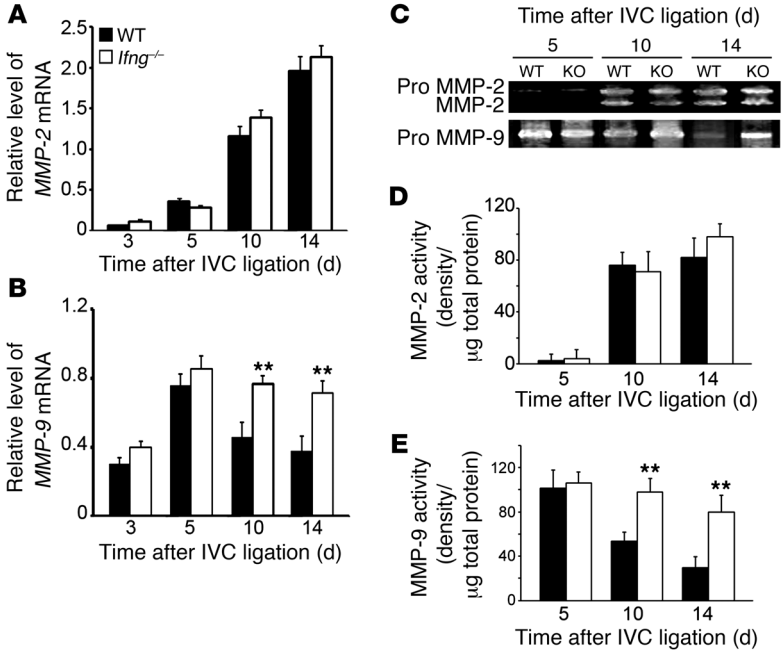

Figure 5
Intrathrombotic MMP-2 and MMP-9 expression. (**A** and **B**) Intrathrombotic gene expression for *MMP-2* (**A**) and *MMP-9* (**B**) in WT and *Ifng*$^{-/-}$ mice was determined by real-time RT-PCR as described in Methods. All values represent the mean ± SEM (n = 6). $^{**}P < 0.01$, *Ifng*$^{-/-}$ versus WT. (**C**–**E**) Intrathrombotic MMP-2 and MMP-9 activities were measured by gelatin gel zymography as described in Methods. Representative gel images from 6 independent experiments are shown in **C**. Gel images were semiquantitatively analyzed; analysis is shown in **D** and **E**. All values represent the mean ± SEM (n = 6). $^{**}P < 0.01$, *Ifng*$^{-/-}$ versus WT.

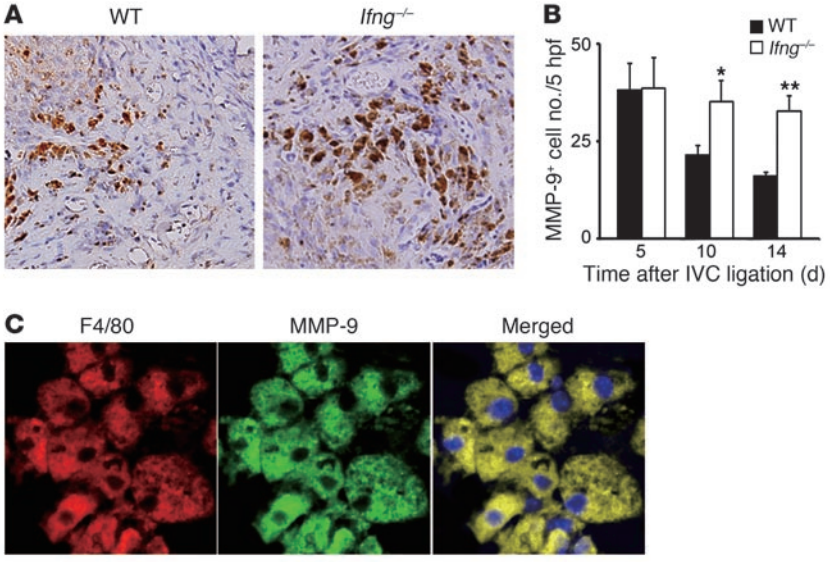

Figure 6
Detection of intrathrombotic MMP-9–positive cells (**A**) Immunohistochemical analysis was performed using anti–MMP-9 pAbs in venous thrombus samples from WT and *Ifng*$^{-/-}$ mice. Representative results from 6 independent experiments are shown here. Original magnification, ×400. (**B**) The numbers of MMP-9–positive cells were determined as described in Methods and are shown in **B**. All values represent the mean ± SEM ($n = 6$ animals). *$P < 0.05$; **$P < 0.01$, *Ifng*$^{-/-}$ versus WT. (**C**) A double-color immunofluorescence analysis of MMP-9–positive cells in the thrombi. The samples were immunostained with the combination of anti-F4/80 mAbs and anti-MMP-9 pAbs, as described in Methods. Representative results from 6 independent experiments are shown here (day 10). Original magnification, ×400. Blue, nuclear staining by DAPI.

tion as revealed by prothrombin time (PT) (control vs. anti–IFN-γ mAbs: 10.8 ± 0.53 s vs. 11.1 ± 0.25 s) and activated partial thromboplastin time (APTT) (control vs. anti–IFN-γ mAbs: 31.3 ± 1.2 s vs. 30.1 ± 0.8 s). These observations demonstrated that IFN-γ blockade was therapeutically effective in accelerating the thrombus resolution without any adverse effects on coagulation function.

Discussion

IFN-γ is produced by Th1 lymphocytes, NK cells, and macrophages (19). Moreover, under several pathological conditions, neutrophils also can produce IFN-γ (20, 22). We proved that macrophage-derived IFN-γ could negatively regulate skin wound healing by dampening the expression of VEGF and TGF-β (23). The resemblance between wound healing and thrombus resolution prompted us to investigate IFN-γ expression in thrombus caused by stasis. Indeed, IFN-γ protein was immunohistochemically detected in venous thrombi obtained from human autopsy cases (Supplemental Figure 1). In the present study, IFN-γ was expressed mainly by infiltrating macrophages and its expression was progressively enhanced until 14 days after the initiation of stasis, suggesting that IFN-γ might be involved in thrombus resolution.

Henke and colleagues previously demonstrated that *Ifng*$^{-/-}$ mice showed similar rates of thrombus resolution in the early phase compared with WT mice, but they did not examine the later phase (18), when intrathrombotic IFN-γ contents were still enhanced in WT mice. Hence, we prolonged the observation period up to 14 days after the initiation of stasis. Although we failed to detect any significant differences in the thrombus mass between WT and *Ifng*$^{-/-}$ mice until 5 days after the initiation of stasis, thrombus mass was significantly reduced in *Ifng*$^{-/-}$ mice compared with WT mice later than 10 days after the initiation of stasis. These observations implied that locally produced IFN-γ might decelerate thrombus resolution in the later phase.

Rats developed significantly larger thrombi when they were rendered neutropenic by the treatment with antipolymorphonuclear leukocyte serum (33). Intrathrombotic neutrophil recruitment was decreased and subsequent thrombus resolution was diminished by genetic disruption of CXCR2, a receptor for CXC chemokines such as CXCL1/KC and CXCL2/MIP-2 with potent chemotactic activities for neutrophils (16). Supporting the notion that macrophage/monocyte recruitment has an important role in thrombus resolution, Ali and colleagues demonstrated that intrathrombus injection of peritoneal macrophages reduced the thrombus size (34). Moreover, the administration of exogenous MCP-1/CCL2, a potent chemoattractant for macrophage, promoted thrombus resolution (17). Conversely, thrombus resolution was impaired with a concomitant reduction in intrathrombotic macrophage recruitment in mice lacking CCR2, a single and specific receptor for CCL2 (18). Thus, these observations indicate that resolution of venous thrombus is regulated by chemokines and subsequent chemokine-mediated neutrophil and/or macrophage recruitment into the thrombi (6–10). In contrast, the absence of IFN-γ failed to affect the intrathrombotic gene expression of CXC and CC chemokines and subsequent leukocyte recruitment. Thus, accelerated thrombus resolution in *Ifng*$^{-/-}$ mice was not directly ascribed to changes in leukocyte recruitment and/or chemokine expression.

Plasmin is formed from plasminogen by the action of tPA and uPA (26–28). This pathway is presumed mainly to regulate fibrin deposition in vascular trees and to activate pericellular fibrinolysis, which is required for cell migration in tissues. Singh and colleagues (35) demonstrated that the absence of uPA impaired thrombus resolution, indicating the essential involvement of plasmin system in thrombus resolution. Evidence is accumulating to indicate that IFN-γ regulated the gene expression of plasminogen activators and their inhibitor (36–39). However, in the present study, there was no significant difference in the intrathrombotic gene expression of *uPA*, *tPA*, and *PAI-1* between WT and *Ifng*$^{-/-}$ mice. Thus, it is unlikely that the absence of IFN-γ could accelerate thrombus resolution by affecting *uPA*, *tPA*, and *PAI-1* expression.

Collagenolysis is indispensable for thrombus resolution (10). Reduced intrathrombotic collagen contents would indicate enhanced collagenolysis in *Ifng*$^{-/-}$ mice compared with WT mice. Among several enzymes with collagenolysis activity, MMP-2 and MMP-9 are presumed to have an important role in collagen turnover during thrombus resolution (18). IFN-γ deficiency increased intrathrombotic *MMP-9* but not *MMP-2* mRNA expression, particularly at the later phase of thrombus resolution. Moreover, MMP-9 activities were higher in *Ifng*$^{-/-}$ mice than WT mice. Transient over-

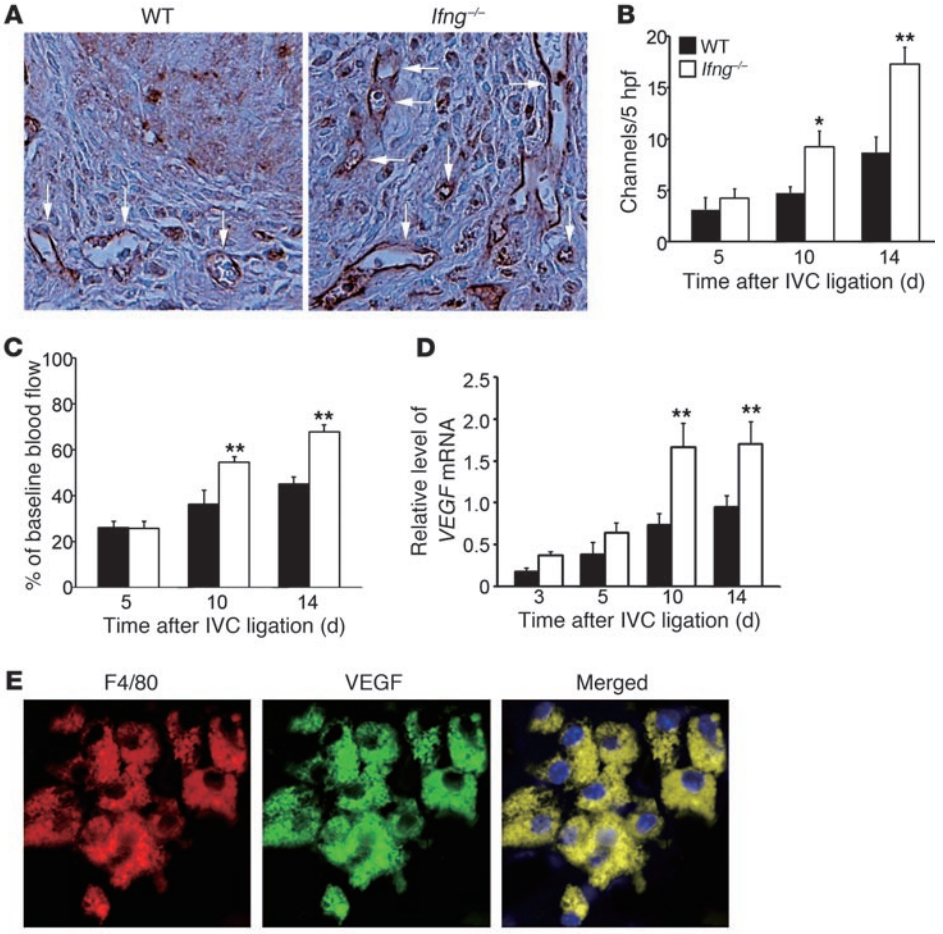

Figure 7

Evaluation of intrathrombotic recanalization. (**A**) Immunohistochemical analysis was performed using anti-vWF pAbs on venous thrombus samples from WT and *Ifng*$^{-/-}$ mice. Original magnification, ×400. Representative results from 6 independent experiments are shown (day 14). Arrows indicate intrathrombotic neovessels. (**B**) The vascular channels were determined as described in Methods. All values represent the mean ± SEM (n = 6 animals). $^{**}P < 0.01$; $^{*}P < 0.05$, *Ifng*$^{-/-}$ versus WT. (**C**) Laser Doppler analysis of thrombosed blood flow. All values represent the mean ± SEM (n = 6 animals). $^{**}P < 0.01$, *Ifng*$^{-/-}$ versus WT. (**D**) Intrathrombotic gene expression of *VEGF* in WT and *Ifng*$^{-/-}$ mice. Real-time RT-PCR was performed as described in Methods. All values represent the mean ± SEM (n = 6). $^{**}P < 0.01$, *Ifng*$^{-/-}$ versus WT. (**E**) A double-color immunofluorescence analysis of VEGF-expressing cells in the thrombus. The samples were immunostained with the combination of anti-F4/80 mAbs and anti-VEGF pAbs as described in Methods. The fluorescent images were digitally merged in the right column. Representative results from 6 independent experiments are shown here. Original magnification, ×400. Blue, nuclear staining by DAPI.

expression of MMP-9 alone could promote intravascular thrombus formation induced by arterial balloon injury, whereas the combination of MMP-9 and tissue inhibitor of metalloproteinase 1 (TIMP-1) could prevent it (32). TIMP-1 expression was enhanced, to a similar extent, in thrombus formation sites of both strains in this model (our unpublished observations), and consequently, enhanced MMP-9 expression in the early phase may have few effects on thrombus formation in the presence of TIMP-1. Alternatively, discrepant observations may arise from the use of different thrombosis models. Nevertheless, retardation of thrombus resolution by an MMP-2/9 inhibitor suggested the potential roles of MMP-9 in thrombus resolution in the later phase when MMP-9 but not MMP-2 expression was higher in *Ifng*$^{-/-}$ than WT mice, although the contribution of MMP-2 cannot be completely excluded.

MMP-9 was expressed predominantly by infiltrating macrophages. Because macrophages are a major target cell of IFN-γ, genetic disruption of IFN-γ could modulate MMP-9 expression by macrophages, similarly reported on several other proinflammatory cytokines, which can regulate *Mmp9* gene expression (40). Ma and colleagues revealed that the IFN-γ/Stat1 signal pathway suppressed *Mmp9* gene expression in human astroglioma and HeLa cell lines (41, 42). In line with this, IFN-γ suppressed PMA-induced *Mmp9* gene expression together with depression of Stat1 activation in murine peritoneal macrophages, while AG490, a JAK2 inhibitor, abrogated these effects. Thus, IFN-γ would prevent macrophages from transcribing the *Mmp9* gene in an autocrine and/or paracrine manner, and IFN-γ deficiency would cancel the suppression, thereby resulting in enhanced MMP-9 expression and subsequent acceleration of collagen degradation in thrombus.

Neovascularization is another key event in the process of thrombus resolution (29–31), as evidenced by retarded thrombus resolution with impaired intrathrombotic neovascularization (16, 18). Several in vitro studies demonstrated that IFN-γ had direct antiangiogenic effects, as evidenced by the inhibition of capillary growth and development (43, 44). In support, we previously observed that *Ifng*$^{-/-}$ mice exhibited enhanced angiogenesis during skin wound healing (23). Likewise, intrathrombotic neovascularization was augmented in *Ifng*$^{-/-}$ mice compared with WT mice. Moreover, MMP-9 also exhibits proangiogenic activity by mediating basement membrane remodeling for endothelialization of tissue matrix (45, 46), and the inhibition of MMP-9 impaired neovascularization in several conditions such as cardiac ischemia (47). Consistently, when WT mice received an MMP-2/9 inhibitor, intrathrombotic recanalization was reduced with no effects on intrathrombotic *Vegf* gene expression, thereby resulting in impaired thrombus resolution. Thus, enhanced MMP-9 expression could promote intrathrombotic recanalization in *Ifng*$^{-/-}$ mice independently of VEGF.

Accumulating evidence indicates that angiogenic growth factors such as VEGF and bFGF are crucial for intrathrombotic neovascularization (48–50). In the present study, the absence or immunoneutralization of IFN-γ augmented *Vegf* gene expression

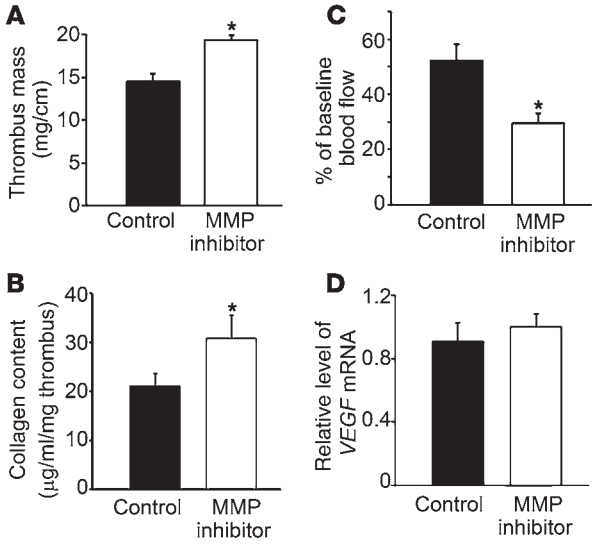

Figure 8
The effects of an MMP inhibitor on thrombus resolution. WT mice were i.p. administered with an MMP inhibitor as described in Methods. At 14 days after the IVC ligation, thrombus weight (**A**) and intrathrombotic collagen contents (**B**), thrombosed blood flow (**C**), and *Vegf* gene expression (**D**) were measured and shown here. All values represent the mean ± SEM (n = 6 animals). *P < 0.05, versus control.

in the thrombi, and MMP inhibitors had no influence on intrathrombotic *Vegf* gene expression. Thus, IFN-γ can negatively regulate *Vegf* gene expression. Kommineni and colleagues demonstrated that IFN-γ suppressed *Vegf* gene expression induced by IL-1β and TNF-α in human corneal epithelial cells (51). Consistently, our study demonstrated that IFN-γ/Stat1 signal pathways attenuated *Vegf* gene expression in murine peritoneal macrophages. Collectively, the absence of IFN-γ promoted intrathrombotic recanalization directly and indirectly.

At present, warfarin is mainly employed against DVT to prevent pulmonary thromboembolism, but this anticoagulation therapy increases the risk of bleeding. *Ifng*$^{-/-}$ mice did not show any abnormalities in coagulation functions but exhibited accelerated thrombus resolution, probably by upregulating the expression of MMP-9 and VEGF, the factors crucially involved in thrombus resolution. Thus, IFN-γ may be efficacious in preventing DVT and its complications. Moreover, IFN-γ blockade also accelerated thrombus resolution without any effects on coagulation function, even if given after thrombus formation. Thus, IFN-γ may be a novel molecular target for the development of therapies that accelerate thrombus resolution in patients with DVT.

Methods

Reagents and Abs. Recombinant mouse IFN-γ and MMP-2/9 inhibitor were purchased from PeproTech and Calbiochem, respectively. PMA and AG490 (a JAK2 inhibitor), were obtained from Sigma-Aldrich. The following mAbs and polyclonal Abs (pAbs) were used for immunohistochemical and double-color immunofluorescence analyses: rat anti-mouse F4/80 mAbs (Dainippon Pharmaceutical Co.), rabbit anti-vWF pAbs (GeneTex), goat anti–IFN-γ pAbs, goat anti-MMP-9 pAbs, goat anti-VEGF pAbs (Santa Cruz Biotechnology Inc.), rabbit anti-phosphorylated–Stat1 (anti–p-Stat1) pAbs (Applied Biological Materials Inc.), rabbit anti-myeloperoxidase (anti-MPO) pAbs (Neomarkers), cyanine dye 3–conjugated (Cy3-conjugated) donkey anti-rat IgG pAbs, and FITC-conjugated donkey anti-rat IgG or goat IgG pAbs (Jackson Immunoresearch Laboratories). For immunoneutralization of endogenous IFN-γ, rat anti-murine IFN-γ mAbs (MAB485, clone: 37895) were purchased from R&D Systems.

Mice. Pathogen-free 8- to 10-week-old male BALB/c mice were obtained from SLC and designated as WT mice in this study. Age- and sex-matched *Ifng*$^{-/-}$ mice, backcrossed to BALB/c mice for at least 8 generations, were used in the following experiments (20). All mice were housed individually in cages under specific pathogen–free conditions during the experiments. All animal experiments were approved by the Committee on Animal Care and Use at Wakayama Medical University.

Stasis-induced DVT model. Intravenous thrombus formation was induced as described previously (18). Briefly, mice were deeply anesthetized by i.p. injection of pentobarbital (50 mg/kg body weight). After a 2-cm incision was made along the abdominal midline, the IVC was ligated with a 3-0 silk suture. In another series of experiments, WT mice were i.p. given anti–IFN-γ mAbs, isotype-matched IgG (50 μg/mouse), or MMP-2/9

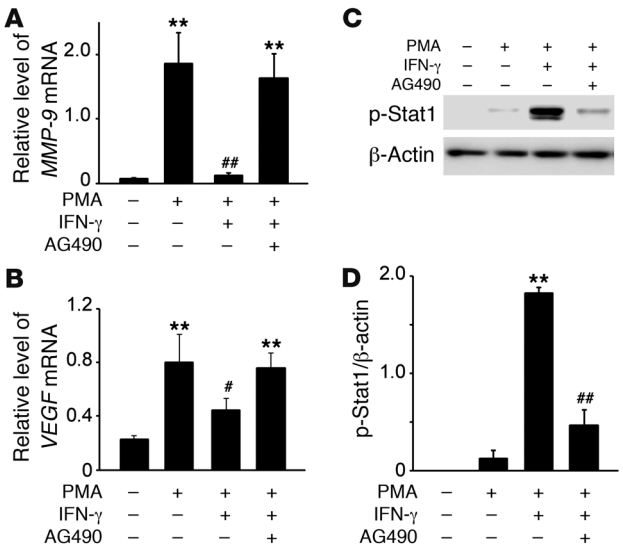

Figure 9
The effects of IFN-γ/Stat1 signal pathways on the gene expression of *MMP-9* and *VEGF* on peritoneal macrophages. Peritoneal macrophages were collected and stimulated as described in Methods. The gene expression of *MMP-9* (**A**) and *VEGF* (**B**) was analyzed by real-time RT-PCR. All values represent the mean ± SEM (n = 6 independent experiments). **P < 0.01, versus no stimulation; ##P < 0.01; #P < 0.05 PMA plus IFN-γ versus PMA alone or PMA plus IFN-γ plus AG490. (**C** and **D**) Western blotting analysis of Stat1 phosphorylation. Representative results from 6 independent experiments are shown in **C**. (**D**) The ratios of phosphorylated Stat1 to β-actin were densitometrically calculated. All values represent the mean ± SEM (n = 6 independent experiments). **P < 0.01, versus no stimulation; ##P < 0.01, PMA plus IFN-γ plus AG490 versus PMA plus IFN-γ.

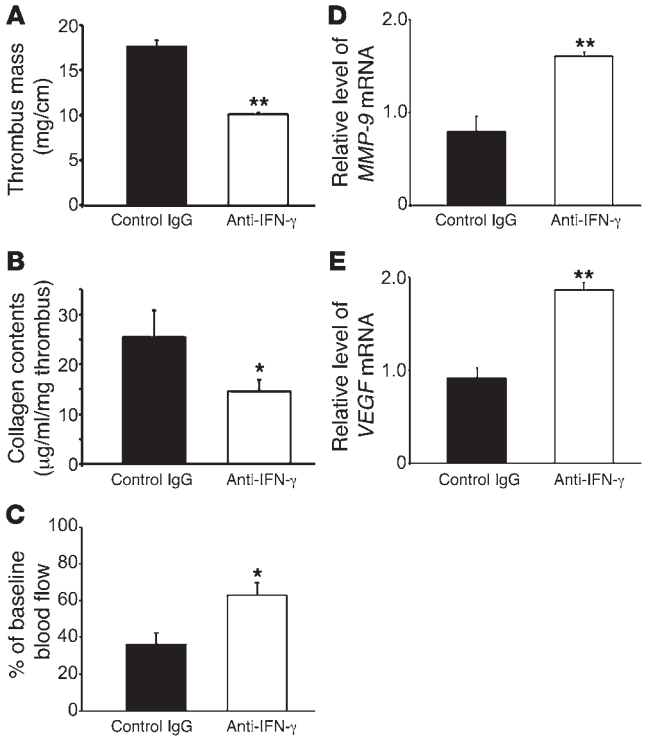

Figure 10
The effects of anti–IFN-γ mAb administration on thrombus resolution. WT mice were i.p. administered anti–IFN-γ mAbs or isotype-matched IgG as described in Methods. At 14 days after the IVC ligation, thrombus weight (**A**) and intrathrombotic collagen contents (**B**), thrombosed blood flow (**C**), and the gene expression of *MMP-9* (**D**) and *VEGF* (**E**) were measured and shown here. All values represent the mean ± SEM ($n = 6$ animals). $^*P < 0.05$; $^{**}P < 0.01$, anti–IFN-γ mAbs versus control IgG.

inhibitor (100 μg/mouse) at 4, 8, and 12 days after the IVC ligation. At the indicated time intervals after the IVC ligation, mice were euthanized by an overdose of diethyl ether and intravenous thrombi were harvested and their weights were measured. We used 6 mice per group and repeated all animal experiments at least 3 times. Because we obtained similar results at each experiment, we demonstrated the representative results from the repeated experiments.

Measurement of PT and APTT. Blood samples were taken with 3.8% citrate solution and centrifuged to obtain plasma samples. PT and APTT of citrated plasma samples were measured by using COAGSEARCH (A&T) according to the manufacturer's instructions.

Histopathological analyses. At the indicated time intervals after the IVC ligation, thrombi were harvested and fixed in 4% formaldehyde buffered with PBS (pH 7.2); paraffin-embedded sections (4-μm thick) were made. The sections were stained with H&E or Masson trichrome solution.

Immunohistochemical analyses. Deparaffinized sections were immersed in 0.3% H_2O_2 in methanol for 30 minutes to eliminate endogenous peroxidase activity. The sections were further incubated with PBS containing 1% normal serum derived from the same species as the origin of the secondary Abs and 1% BSA to reduce nonspecific reactions. The sections were incubated with anti-MPO pAbs, anti-F4/80 mAbs, anti-vWF pAbs, or anti-MMP-9 pAbs at a concentration of 1 μg/ml at 4°C overnight. After the incubation of biotinylated secondary Abs, immune complexes were visualized using the Catalyzed Signal Amplification System (Dako) according to the manufacturer's instructions.

Measurements of leukocytes and neovessels. Intrathrombotic leukocytes and vascular density were semiquantitatively evaluated. Briefly, after MPO-positive neutrophils, F4/80-positive macrophages or MMP-9–positive cells were enumerated in 5 high-power fields (×1,000) within the thrombus, total numbers in the 5 fields were combined. Intrathrombotic vWF-positive neovessels with tube-like formation were counted in 5 high-power fields (×1,000), as described previously (18). All measurements were performed by an examiner without a prior knowledge of the experimental procedures.

A double-color immunofluorescence analysis. Deparaffinized sections or peritoneal macrophages were incubated with PBS containing 1% normal donkey serum and 1% BSA to reduce nonspecific reactions as previously described (23). Thereafter, the sections were further incubated in the combination of anti-F4/80 and anti–IFN-γ, anti-F4/80 and anti–MMP-9, anti-F4/80 and anti–p-Stat1, or anti-F4/80 and anti-VEGF. All Abs were used at a concentration of 1 μg/ml. After the incubation with fluorochrome-conjugated secondary Abs (15 μg/ml) at room temperature for 30 minutes, the sections were observed under fluorescence microscopy. In some experiments, nuclei were stained using DAPI (Roche Diagnostics) according to the manufacturer's instructions.

IVC blood flow measurement by a laser Doppler. Microvascular IVC blood flow was assessed by laser Doppler imaging (OMEGA-FLO FLO-C1 BV, OMEGAWAVE) as described previously (18). After laparotomy, at pre-IVC ligation, immediate postligation, and at harvest, blood flow through the exposed IVC region of interest was assessed; a 5-second scan with 30-second interval over 4 scanning cycles was performed. Depth was constant and was adjusted for each mouse to ensure the best estimation of the midcoronal IVC section. These scans were saved, and accompanying image software was used to estimate the mean color flow by using a standardized area of analysis. The intensities were reported as percentage of baseline blood flows, specific to each animal to ensure consistency.

Measurement of intrathrombotic hydroxyproline contents. At the indicated time intervals after IVC ligation, venous thrombi were removed and dried for 16 hours at 120°C. Hydroxyproline (HP), a major constituent of collagen, was measured as an index of collagen accumulation at the thrombi, as described previously (23). HP content was calculated by comparison with standards and expressed as the amount (μg) per dry weight of thrombus (mg).

Table 1
Sequences of the primers used for real-time RT-PCR

Transcript	Sequence
Ifng	(F) 5′-CGGCACAGTCATTGAAAGCCTA-3′
	(R) 5′-GTTGCTGATGGCCTGATTGTC-3′
Mmp2	(F) 5′-GATAACCTGGATGCCGTCGTG-3′
	(R) 5′-CTTCACGCTCTTGAGACTTTGGTTC-3′
Mmp9	(F) 5′-GCCCTGGAACTCACACGACA-3′
	(R) 5′-TTGGAAACTCACACGCCAGAAG-3′
Vegf	(F) 5′-GAGGATGTCCTCACTCGGATG-3′
	(R) 5′-GTCGTGTTTCTGGAAGTGAGCAA-3′
uPA	(F) 5′-GAGCAGCTCATCTTGCACGAATAC-3′
	(R) 5′-GCCAGTGATCTCACAGTCTGAACC-3′
tPA	(F) 5′-AAGTGGTCTTGGGCAGAACATACAG-3′
	(R) 5′-TCTTGGGCACATTGCTTGGA-3′
Pai1	(F) 5′-TTCCAAGGCATCCAGAAGCAG-3′
	(R) 5′-CCGGAAATGACACATTGAAGTGAG-3′
β-*actin*	(F) 5′-CATCCGTAAAGACCTCTATGCCAAC-3′
	(R) 5′-ATGGAGCCACCGATCCACA-3′

F, forward primer; R, reverse primer.

Collagen assay. Thrombus collagen content was estimated by a commercially available kit according to the manufacturer's instructions (Bicolor), as described (18). Collagen amount was then corrected to thrombus weight for each sample (μg/ml/mg of thrombus).

Extraction of total RNAs and real-time RT-PCR. Real-time RT-PCR was performed as described previously (52). Briefly, total RNA was extracted from tissue samples (100 μg) using ISOGEN (Nippon Gene) according to the manufacturer's instructions, and 5 μg of total RNA was reverse transcribed into cDNA at 42°C for 1 hour in 20 μl reaction mixture containing mouse Moloney leukemia virus reverse transcriptase (PrimeScript; Takara Bio) with random 6 primers (Takara Bio). Thereafter, generated cDNA was subjected to real-time PCR analysis using SYBR Premix Ex Taq II kit (Takara Bio) with the specific primers sets (Table 1 and Supplemental Table 1). Relative quantity of target gene expression to β-actin gene was measured by comparative Ct method.

ELISA for IFN-γ. Thrombus samples were obtained at the indicated time intervals and were homogenized with 0.3 ml of PBS (pH 7.2) containing Complete Protease Inhibitor Mixture (Roche Diagnostics). The homogenates were centrifuged at 12,000 *g* for 15 minutes. IFN-γ levels in the supernatant were measured using a specific ELISA kit (R&D Systems), according to the manufacturer's instructions. The detection limit was greater than 2 pg/ml. Total protein in the supernatant was measured with a commercial kit (BCA Protein Assay Kit; Pierce) using BSA as a standard. The data were expressed as IFN-γ (ng/ml)/total protein (mg/ml) for each sample.

Gelatin SDS-PAGE substrate zymography. The intrathrombotic activities of MMP-2 and MMP-9 were determined by the Gelatin-Zymography Kit (Primary Cell) according to the manufacturer's instructions. The data were expressed as band intensity/μg total protein.

Cell culture. WT mice were i.p. injected with 2 ml of 3% thioglycolate (Sigma-Aldrich), and i.p. macrophages were harvested (macrophage purity > 95%) 3 days later as described previously (53). The cells were suspended in antibiotic-free RPMI 1640 medium containing 10% FBS and incubated at 37°C in three 24-well cell culture plates. Two hours later, nonadherent cells were removed, and the medium was replaced. After the cells were stimulated with PMA (50 ng/ml), PMA (50 ng/ml) plus IFN-γ (500 U/ml), or PMA (50 ng/ml) plus IFN-γ (500 U/ml) plus AG490 (100 nM) for 24 hours, the cells were subjected to subsequent analyses.

Western blotting. The isolated macrophages were homogenized with a lysis buffer (20 mM Tris-HCl [pH 7.6], 150 mM NaCl, 1% Triton X-100, 1 mM EDTA) containing Complete Protease Inhibitor Cocktail (Roche) and phosphatase inhibitor cocktails for serine/threonine protein phosphatases and tyrosine protein phosphatases (P2850 and P5726; Sigma-Aldrich) and were centrifuged to obtain lysates. The lysates (equivalent to 30 μg protein) were electrophoresed in a 10% SDS-polyacrylamide gel and transferred onto a nylon membrane. After the membrane was sequentially incubated with optimally diluted primary Abs and HRP-conjugated secondary Abs, the immune complexes were visualized using the ECL system (Amersham Biosciences). The band intensities were measured using NIH Image Analysis Software version 1.61 (NIH) and were calculated as the ratios to β-actin.

Statistics. The means and SEMs were calculated for all parameters determined in this study. Statistical significance was evaluated by using ANOVA or Mann-Whitney *U* test. $P < 0.05$ was accepted as statistically significant.

Acknowledgments

We thank Yoichiro Iwakura (University of Tokyo, Tokyo, Japan) for providing us with *Ifng*$^{-/-}$ mice. This study was financially supported in part by Grants-in-Aids for Scientific Research from the Ministry of Education, Culture, Science, and Technology of the Japanese government.

Received for publication January 24, 2011, and accepted in revised form April 20, 2011.

Address correspondence to: Toshikazu Kondo, Department of Forensic Medicine, Wakayama Medical University, 811-1 Kimiidera, Wakayama 641-8509, Japan. Phone: 81.73.441.0641; Fax: 81.73.441.0641; E-mail: kondot@wakayama-med.ac.jp.

1. Bates SM, Ginsberg JS. Clinical practice. Treatment of deep-vein thrombosis. *N Engl J Med*. 2004; 351(3):268–277.
2. Rosendaal FR. Venous thrombosis: a multicausal disease. *Lancet*. 1999;353(9159):1167–1173.
3. Kearon C. Epidemiology of venous thromboembolism. *Semin Vasc Med*. 2001;1(1):7–26.
4. Coon WW, Willis PW 3rd, Keller JB. Venous thromboembolism and other venous disease in the Tecumseh community health study. *Circulation*. 1973; 48(4):839–846.
5. Anderson FA Jr, et al. A population-based perspective of the hospital incidence and case-fatality rates of deep vein thrombosis and pulmonary embolism. The Worcester DVT Study. *Arch Intern Med*. 1991; 151(5):933–938.
6. Peterson KL. Acute pulmonary thromboembolism: has its evolution been redefined? *Circulation*. 1999;99(10):1280–1283.
7. Shebuski RJ, Kilgore KS. Role of inflammatory mediators in thrombogenesis. *J Pharmacol Exp Ther*. 2002;300(3):729–735.
8. Lambert MP, Sachais BS, Kowalska MA. Chemokines and thrombogenicity. *Thromb Haemost*. 2007; 97(5):722–729.
9. Wakefield TW, Henke PK. The role of inflammation in early and late venous thrombosis: Are there clinical implications? *Semin Vasc Surg*. 2005;18(3):118–129.
10. Wakefield TW, Myers DD, Henke PK. Mechanisms of venous thrombosis and resolution. *Arterioscler Thromb Vasc Biol*. 2008;28(3):387–391.
11. Cines DB, et al. Endothelial cells in physiology and in the pathophysiology of vascular disorders. *Blood*. 1998;91(10):3527–3561.
12. Wakefield TW, et al. Venous thrombosis-associated inflammation and attenuation with neutralizing antibodies to cytokines and adhesion molecules. *Arterioscler Thromb Vasc Biol*. 1995;15(2):258–268.
13. Stewart GJ. Neutrophils and deep venous thrombosis. *Haemostasis*. 1993;23(suppl 1):127–140.
14. Granger DN, Kubes P. The microcirculation and inflammation: modulation of leukocyte-endothelial cell adhesion. *J Leukoc Biol*. 1994;55(5):662–675.
15. Tan P, Luscinskas FW, Homer-Vanniasinkam S. Cellular and molecular mechanisms of inflammation and thrombosis. *Eur J Vasc Endovasc Surg*. 1999;17(5):373–389.
16. Henke PK, et al. Deep vein thrombosis resolution is modulated by monocyte CXCR2-mediated activity in a mouse model. *Arterioscler Thromb Vasc Biol*. 2004; 24(6):1130–1137.
17. Humphries J, McGuinness CL, Smith A, Waltham M, Poston R, Burnand KG. Monocyte chemotactic protein-1 (MCP-1) accelerates the organization and resolution of venous thrombi. *J Vasc Surg*. 1999; 30(5):894–899.
18. Henke PK, et al. Targeted deletion of CCR2 impairs deep vein thombosis resolution in a mouse model. *J Immunol*. 2006;177(5):3388–3397.
19. Farrar MA, Schreiber RD. The molecular cell biology of interferon-γ and its receptor. *Annu Rev Immunol*. 1993;11:571–611.
20. Hayashi T, Ishida Y, Kimura A, Iwakura Y, Mukaida N, Kondo T. IFN-γ protects cerulein-induced acute pancreatitis by repressing NF-κB activation. *J Immunol*. 2007;178(11):7385–7394.
21. Kimura A, et al. Interferon-γ plays protective roles in sodium arsenite-induced renal injury by up-regulating intrarenal multidrug resistance-associated protein 1 expression. *Am J Pathol*. 2006;169(4):1118–1128.
22. Ishida Y, et al. Essential involvement of IFN-γ in *Clostridium difficile* toxin A-induced enteritis. *J Immunol*. 2004;172(5):3018–3025.
23. Ishida Y, Kondo T, Takayasu T, Iwakura Y, Mukaida N. The essential involvement of cross-talk between IFN-γ and TGF-β in the skin wound-healing process. *J Immunol*. 2004;172(3):1848–1855.
24. Ishida Y, Kondo T, Ohshima T, Fujiwara H, Iwakura Y, Mukaida N. A pivotal involvement of IFN-gamma in the pathogenesis of acetaminophen-induced acute liver injury. *FASEB J*. 2002; 16(10):1227–1236.
25. Tsuji H, et al. Alleviation of lipopolysaccharide-induced acute liver injury in Propionibacterium acnes-primed IFN-γ-deficient mice by a concomitant reduction of TNF-α, IL-12, and IL-18 production. *J Immunol*. 1999;162(2):1049–1055.
26. Tabrizi P, et al. Tissue plasminogen activator (tPA) deficiency exacerbates cerebrovascular fibrin deposition and brain injury in a murine stroke model: studies in tPA-deficient mice and wild-type mice on a matched genetic background. *Arterioscler Thromb Vasc Biol*. 1999;19(11):2801–2806.
27. Bugge TH, et al. Urokinase-type plasminogen activator is effective in fibrin clearance in the absence of its receptor or tissue-type plasminogen activator. *Proc Natl Acad Sci U S A*. 1996;93(12):5899–5904.
28. Ploplis VA, French EL, Carmeliet P, Collen D, Plow EF. Plasminogen deficiency differentially affects

recruitment of inflammatory cell populations in mice. *Blood*. 1998;91(6):2005–2009.
29. Modarai B, Burnand KG, Humphries J, Waltham M, Smith A. The role of neovascularisation in the resolution of venous thrombus. *Thromb Haemost*. 2005; 93(5):801–809.
30. Wakefield TW, et al. Neovascularization during venous thrombosis organization: a preliminary study. *J Vasc Surg*. 1999;30(5):885–892.
31. Henke PK, et al. Interleukin-8 administration enhances venous thrombosis resolution in a rat model. *J Surg Res*. 2001;99(1):84–91.
32. Morishige K, et al. Overexpression of matrix metalloproteinase-9 promotes intravascular thrombus formation in porcine coronary arteries in vivo. *Cardiovasc Res*. 2003;57(2):572–585.
33. Varma MR, et al. Neutropenia impairs venous thrombosis resolution in the rat. *J Vasc Surg*. 2003; 38(5):1090–1098.
34. Ali T, et al. Monocyte recruitment in venous thrombus resolution. *J Vasc Surg*. 2006;43(3):601–608.
35. Singh I, et al. Failure of thrombus to resolve in urokinase-type plasminogen activator gene-knockout mice: rescue by normal bone marrow-derived cells. *Circulation*. 2003;107(6):869–875.
36. Arnman V, Stemme S, Rymo L, Risberg B. Interferon-gamma modulates the fibrinolytic response in cultured human endothelial cells. *Thromb Res*. 1995; 77(5):431–440.
37. Gyetko MR, Shollenberger SB, Sitrin RG. Urokinase expression in mononuclear phagocytes: cytokine-specific modulation by interferon-γ and tumor necrosis factor-α. *J Leukoc Biol*. 1992;51(3):256–263.
38. Gallicchio M, Hufnagl P, Wojta J, Tipping P. IFN-γ inhibits thrombin- and endotoxin-induced plasminogen activator inhibitor type 1 in human endothelial cells. *J Immunol*. 1996;157(6):2610–2617.
39. Kosaka H, Yoshimoto T, Yoshimoto T, Fujimoto J, Nakanishi K. Interferon-γ is a therapeutic target molecule for prevention of postoperative adhesion formation. *Nat Med*. 2008;14(4):437–441.
40. Yan C, Boyd DD. Regulation of matrix metalloproteinase gene expression. *J Cell Physiol*. 2007; 211(1):19–26.
41. Ma Z, Qin H, Benveniste EN. Transcriptional suppression of matrix metalloproteinase-9 gene expression by IFN-γ and IFN-β: critical role of STAT-1α. *J Immunol*. 2001;167(9):5150–5159.
42. Ma Z, Chang MJ, Shah RC, Benveniste EN. Interferon-γ-activated STAT-1α suppresses MMP-9 gene transcription by sequestration of the coactivators CBP/p300. *J Leukoc Biol*. 2005;78(2):515–523.
43. Sato N, et al. Actions of TNF and IFN-γ on angiogenesis in vitro. *J Invest Dermatol*. 1990; 95(6 suppl):85S–89S.
44. Maheshwari RK, Srikantan V, Bhartiya D, Kleinman HK, Grant DS. Differential effects of interferon gamma and alpha on in vitro model of angiogenesis. *J Cell Physiol*. 1991;146(1):164–169.
45. Visse R, Nagase H. Matrix metalloproteinases and tissue inhibitors of metalloproteinases: structure, function, and biochemistry. *Circ Res*. 2003; 92(8):827–839.
46. Whatling C, McPheat W, Hurt-Camejo E. Matrix management: assigning different roles for MMP-2 and MMP-9 in vascular remodeling. *Arterioscler Thromb Vasc Biol*. 2004;24(1):10–11.
47. Ducharme A, et al. Targeted deletion of matrix metalloproteinase-9 attenuates left ventricular enlargement and collagen accumulation after experimental myocardial infarction. *J Clin Invest*. 2000; 106(1):55–62.
48. Modarai B, et al. Adenovirus-mediated VEGF gene therapy enhances venous thrombus recanalization and resolution. *Arterioscler Thromb Vasc Biol*. 2008; 28(10):1753–1759.
49. Waltham M, Burnand K, Fenske C, Modarai B, Humphries J, Smith A. Vascular endothelial growth factor naked DNA gene transfer enhances thrombus recanalization and resolution. *J Vasc Surg*. 2005; 42(6):1183–1189.
50. Waltham M, Burnand KG, Collins M, Smith A. Vascular endothelial growth factor and basic fibroblast growth factor are found in resolving venous thrombi. *J Vasc Surg*. 2000;32(5):988–996.
51. Kommineni VK, Nagineni CN, William A, Detrick B, Hooks JJ. IFN-γ acts as anti-angiogenic cytokine in the human cornea by regulating the expression of VEGF-A and sVEGF-R1. *Biochem Biophys Res Commun*. 2008;374(3):479–484.
52. Inui M, Ishida Y, Kimura A, Kuninaka Y, Mukaida N, Kondo T. Protective roles of CX3CR1-mediated signals in toxin A-induced enteritis through the induction of heme oxygenase-1 expression. *J Immunol*. 2011;186(1):423–431.
53. Ishida Y, et al. Essential involvement of CX3CR1-mediated signals in the bactericidal host defense during septic peritonitis. *J Immunol*. 2008; 181(6):4208–4218.